

# Loop Current warming by Hurricane Wilma

L.-Y. Oey,<sup>1</sup> T. Ezer,<sup>1</sup> D.-P. Wang,<sup>2</sup> S.-J. Fan,<sup>3</sup> and X.-Q. Yin<sup>1,4</sup>

Received 27 January 2006; revised 8 March 2006; accepted 17 March 2006; published 29 April 2006.

[1] Hurricanes mix and cool the upper ocean, as shown here in observations and modeling of the Caribbean Sea and the Gulf of Mexico during the passage of hurricane Wilma. Curiously, the upper ocean around the Loop Current warmed prior to Wilma's entrance into the Gulf. The major cause was increased volume and heat transports through the Yucatan Channel produced by storm-induced convergences in the northwestern Caribbean Sea. Such oceanic variability may have important impacts on hurricane predictions. **Citation:** Oey, L.-Y., T. Ezer, D.-P. Wang, S.-J. Fan, and X.-Q. Yin (2006), Loop Current warming by Hurricane Wilma, *Geophys. Res. Lett.*, 33, L08613, doi:10.1029/2006GL025873.

## 1. Introduction

[2] Wilma (Oct/16~26/2005) is the most powerful Atlantic hurricane on record. The storm's minimum surface pressure was 882 mb and its maximum surface wind speeds  $|u_a|$  was  $78 \text{ m s}^{-1}$  (<http://www.nhc.noaa.gov/>) (Figure 1). The storm formed southwest of Jamaica near a warm eddy with high ocean heat content (OHC) (Figure 1) [Leipper and Volgenau, 1972]. It strengthened on Oct/18/15Z ( $|u_a| \approx 34 \text{ m s}^{-1}$ ), and became a category-5 hurricane on Oct/19/09Z as it moved west/northwestward over a high OHC region in the Cayman Sea. Wilma weakened as it made landfall on Oct/22/06Z at Cozumel Island and Yucatan peninsula, but  $|u_a|$  was still  $>60 \text{ m s}^{-1}$ . It weakened further ( $|u_a| \approx 45 \text{ m s}^{-1}$ ) while it moved slowly overland, and strengthened some 24 ~ 30 hours later as it passed over the warm Loop Current ( $|u_a| \approx 56 \text{ m s}^{-1}$  on Oct/24) on its way to Florida.

[3] Wilma is one of the few major hurricanes to directly hit the Yucatan Channel, (<http://www.nhc.noaa.gov/pastall.shtml>) and is also the only such hurricane to have remained in the northwestern Cayman Sea (west of  $79^\circ\text{W}$ ) and the Yucatan Channel for a long 7-day period. (Hurricanes Emily (11–21/Jul/2005) came near the Yucatan Channel; other hurricanes are Ivan in 2004, Isidore and Lili both in 2002, Allen in 1980, Isbell in 1964, Carla in 1961, and Florence in 1953.) While the storm was in the Caribbean Sea, its progression speed  $U$  was  $2.5 \sim 3 \text{ m s}^{-1}$ , and  $U > C$  (where  $C$  is the first-mode oceanic baroclinic wave speed,  $\approx 2.5 \text{ m s}^{-1}$ ) [Chelton et al., 1998]. Such a storm ( $U > C$ ) produces lee waves with large vertical isopycnal movements

( $>50 \text{ m}$ ; vertical velocity  $w \approx \pm 10^{-3} \text{ m s}^{-1}$ ) in the ocean and no disturbances ahead [Geisler, 1970]. The combined action of upwelling and mixing is effective in cooling the upper ocean near the storm's eye especially for a slowly-moving storm [Price, 1981]. Mixing alters the OHC that in turn can modify the storm. On the other hand, less is known about the effects of a hurricane on the powerful Loop Current, where strong horizontal advection may defy interpretations based on vertical motions alone. (See Oey et al. [2005a] for a review of the Loop Current and general circulation in the Gulf of Mexico).

## 2. Methodology

[4] To analyze the upper-ocean changes caused by Wilma, we use data from the National Data Buoy Center (NDBC; <http://www.ndbc.noaa.gov/>), including SST (at  $z = -1 \text{ m}$ ) and meteorological observations (Figure 1 shows buoy locations). We also use results of an ocean forecast (the "control" run) for the Caribbean Sea and the Gulf of Mexico [e.g., Oey et al., 2005b]. Though we estimate large surface heat losses (peak  $\approx 1300 \text{ J m}^{-2}\text{s}^{-1}$  at 42056, and  $800 \text{ J m}^{-2}\text{s}^{-1}$  at 42057; see hurricane Opal [Shay et al., 2000]), these have small effects in decreasing the temperatures of the upper ocean, which is cooled more by mixing [Price, 1981].

[5] The forecast is initialized with a nowcast ocean field (Loop Current and eddies) that has already been assimilated with satellite data up to Oct/16/2005, after which the model is run through Nov/06/2005 without data assimilation. Oey et al. [2005a, 2005b] and references quoted therein give details of the model and the data assimilation scheme. Besides the 'control' run, other auxiliary runs are also conducted using different wind and initial density fields as will be pointed out below. The original forecast used Global Forecast System winds [Caplan et al., 1997], but the model was rerun for this study using also the high-resolution analyzed winds (available at <http://www.aoml.noaa.gov/hrd/>). This rerun is still referred to as "forecast" to emphasize that it is free from satellite data assimilation. Wind stresses were computed using a bulk formula. We use a drag coefficient ( $C_d$ ) that curve-fits data for low-to-moderate winds [Large and Pond, 1981] with data for high wind speeds [Powell et al., 2003]:

$$C_d \times 10^3 = \begin{cases} 1.2, & W \leq 11 \text{ m s}^{-1}; \\ 0.49 + 0.065 W, & 11 < W \leq 19 \text{ m s}^{-1}; \\ 1.364 + 0.0234 W - 0.0002 W^2, & 19 < W \leq 100 \text{ m s}^{-1}, \end{cases} \quad (1)$$

<sup>1</sup>Atmospheric and Oceanic Sciences, Princeton University, Princeton, New Jersey, USA.

<sup>2</sup>Marine Sciences Research Center, Stony Brook University, Stony Brook, New York, USA.

<sup>3</sup>Stevens Institute of Technology, Hoboken, New Jersey, USA.

<sup>4</sup>The First Institute of Oceanography, Qingdao, China.

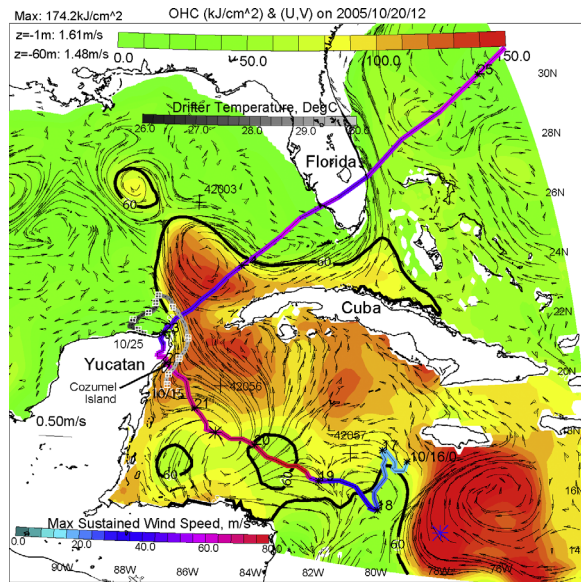


**Figure 1.** A color image of the forecast  $OHC$  on Oct/20/12GMT/2005 (color-scale across top) during hurricane Wilma. Maximum  $OHC$  (blue asterisk south of Jamaica) is printed on the top-left corner of the page. Thick-black contour indicates  $OHC = 60 \text{ kJ/cm}^2$ . Forecast currents at  $z = -1 \text{ m}$  are shown as black trajectories (with arrows) launched from every other four grid points. Maximum speeds (which occurred in Yucatan Channel) at  $z = -1 \text{ m}$  and  $-60 \text{ m}$  are printed. Wilma's path is shown colored with its maximum sustained wind speeds (color-scale at bottom-left). Numbers at the small asterisks indicate days in October and the large asterisk the position of the storm corresponding to this forecast date. Off the Yucatan coast, the path of an observed drifter shaded with temperature (scale across "Florida") are marked daily with a crossed-square, from Oct/15 to Oct/25. Positions of the three NDBC stations are marked with plus signs.

where  $W$  is the wind speed. Surface heat and evaporative fluxes were set to zero, so that changes in the model ocean temperatures are due to its internal dynamics.

### 3. Results

[6] To account for wind mixing on the  $OHC$  of an evolving ocean, a non-dimensional parameter  $\Phi$  is used, where  $\Phi$  is obtained by estimating the energy required to mix water in an upper layer of depth  $Z_{26}$  with the cooler water in a subsurface layer of depth  $h$ , and comparing this energy to power dissipation by the wind:

$$\Phi = \left( \frac{1}{2} g h Z_{26} \Delta \rho \right) / \left( \gamma \int_0^{\tau} \rho_a C_d W^3 dt \right). \quad (2)$$

[7] Here,  $Z_{26}$  is taken as the depth of the  $26^\circ\text{C}$  isotherm,  $\Delta \rho$  is the initial density difference between the two layers ( $\approx 1 \sim 2 \text{ kg m}^{-3}$  from the model),  $\gamma$  is the efficiency of work done by the wind,  $\tau$  is a wind time scale,  $\rho_a$  is air density,  $t$  is time and  $g$  is acceleration due to gravity. Figures 2b and 2c show observed and forecast sea-surface

temperatures ( $SST$ 's; at  $z = -1 \text{ m}$ ) and  $\log_{10}$  of  $\Phi \approx g(Z_{26})^2 / \alpha W^3$ , where we have set  $h \approx Z_{26}$  in (2) and  $\alpha$  is then a time scale proportional to the duration of the wind forcing [Turner, 1973]. For plotting convenience, we set  $\alpha = 1 \text{ s}$  and assume a constant  $Z_{26} = 100 \text{ m}$ . The  $SST$  should decrease with  $\Phi$  if the dominant cooling is due to stirring by the hurricane. Figure 2 shows minimum  $SST$ 's on Oct/19–20 at 42057 and on Oct/21–22 at 42056 following minima in  $\Phi$ , with lags of about  $1 \sim 2 \text{ days}$ . The decrease in  $SST$  at 42057 (Figure 2c) began on Oct/17, a short time after Wilma formed. With the chosen parameters,  $\Phi \approx 100$  appears to be an approximate critical value below which wind mixing is sufficiently strong to cool the upper ocean. The large drop on Oct/19–20 was caused by the sudden intensification of Wilma, even though the storm was moving farther west. The model forecasted the large drop in  $SST$  but lost its predictability beyond Oct/26.

[8] The  $SST$  at 42056 (Figure 2b) decreased on Oct/18 ~ 19 while Wilma's center was still some  $400 \sim 600 \text{ km}$  to the east; the decrease in  $SST$  follows a decrease in  $\Phi \leq 100$ . A careful examination of satellite sea-surface height anomaly ( $SSHA$ ) (AVISO; available at [www.aviso.oceanobs.com](http://www.aviso.oceanobs.com)) data indicated no cold eddies nearby, so the cooling was most likely caused by mixing. By Oct/21 when the storm center was nearest to 42056, the  $SST$  had already dropped by  $0.5^\circ\text{C}$ , and  $SST$  decreased by another  $0.9^\circ\text{C}$  through Oct/

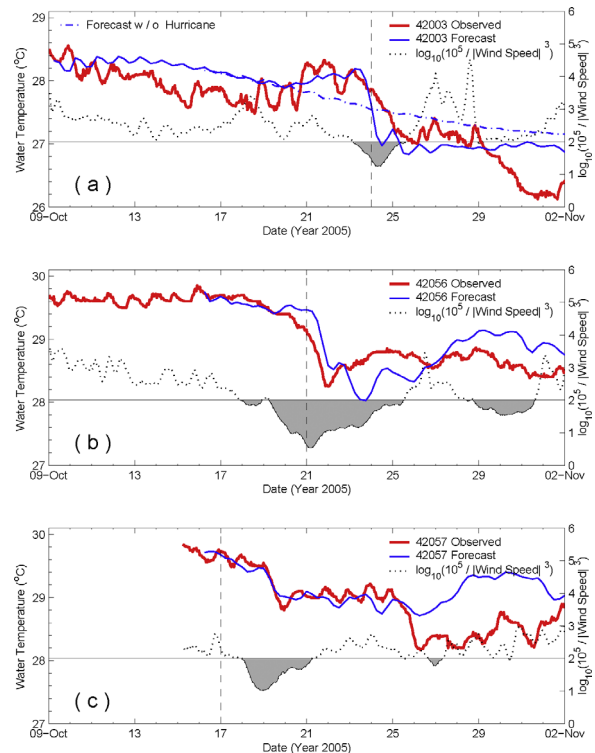


**Figure 2.** Observed (red solid) and forecast (blue solid)  $SST$  (at  $z = -1 \text{ m}$ ) at NDBC stations (a) 42003, (b) 42056 and (c) 42057 during hurricane Wilma. The dotted curve in each panel is ( $\log_{10}$  of) the inverse wind power dissipation (see text); shaded are values  $\leq 2$ . The dash-dot curve in Figure 1a is  $SST$  for auxiliary model run A1 in which Wilma is turned off. The vertical dashed line in each panel indicates time when Wilma is closest to the respective station.

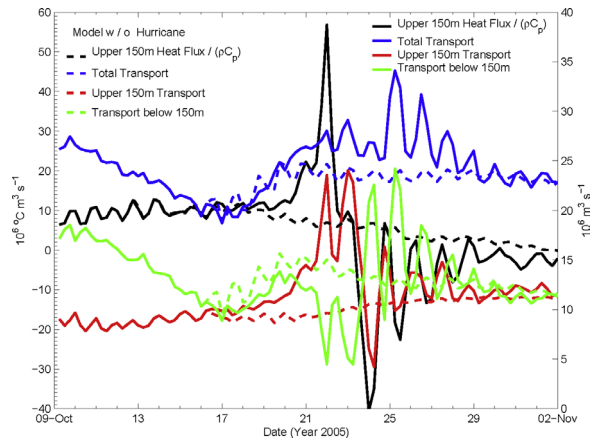


**Figure 3.** Model volume (right-side scale) and heat transports ( $\rho_o C_p$ ) through the Yucatan Channel during Wilma. Solid curves are for model with Wilma; dashed curves are without Wilma. The upper 150 m heat flux is defined as  $\rho_o C_p \int \mathbf{v} \cdot \mathbf{n} (T - 26) dx dz$ , where  $\mathbf{v}$  is the velocity normal to the transect,  $T$  is temperature, and vertical integration is from  $z = -150$  m to the surface.

22. It is common for *SST* to decrease prior to the arrival of a hurricane, but that usually occurs within hours and in close proximity (100 ~ 200 km) of the storm's center [Price, 1981; Shay et al., 2000]. In the case of Wilma, the slowness of the storm combines with its intensity and large size to produce winds that mixed and cooled the upper ocean hundreds of kilometers ahead of the storm's center. The forecast *SST* shows a similar (but less dramatic) “remote” effect; it also shows the large decrease when the storm center passes. The model loses its predictability at 42056 beyond about Oct/30.

[9] Cooling ahead of the storm also exists in the Loop Current especially in its core. However, strong advection around the Loop complicates the picture. Buoy 42003 is located in close proximity of the Loop. The  $\Phi$  in Figure 2a suggests that wind mixing at 42003 played a minor role ( $\Phi > 100$ ) prior to Wilma's arrival on Oct/23 ~ 24. The observed *SST* first decreased to a minimum on Oct/19 ~ 20; it then increased by about 0.4°C from Oct/20 through Oct/23 before dropping sharply (−0.8°C) on Oct/23 ~ 25 as Wilma passed south of the site. This final sharp drop is caused partly by wind-mixing (the  $\Phi$  drops below 100), and partly by advection of cooler shelf/slope waters as Wilma moved toward Florida (not shown). The sharp drop agrees well with along-track data on Oct/24/15GMT from satellite *ENVISAT* (www.aoml.noaa.gov/phod/dataphod), which flew almost exactly over 42003 on that date and recorded a minimum *SSHA*  $\approx -0.3$  m. The initial decrease to the minimum *SST* on Oct/19 (Figure 2a) seems to be part of the natural (i.e., unrelated to Wilma) variability of the Loop Current, since the *SST* for the auxiliary run A1 (without Wilma) shows a similar decrease. However, the subsequent ~3-day (Oct/20 ~ 23) warming is unique for 42003. No such *SST*-rise was observed at 42056 and 42057 (Figures 2b and 2c), nor have similar phenomena been observed previously. The forecast (Figure 2a) shows a similar *SST*-variation of the rise of *SST* on Oct/20 ~ 23 and the subsequent sharp drop. In contrast, the *SST* decreases monotonically with time in the auxiliary run.

[10] The 3-day *SST*-rise prior to Wilma's entrance into the Gulf could have been induced by passage of an isolated warm feature. While this could not be ruled out (objective-analysis *SSH* (OASSH; AVISO) maps based on altimetry data did not show such a feature), the model suggests an alternative explanation. Temperatures at other locations around the perimeter of the (model) Loop show a similar rise, suggesting a more wide-spread process that links Wilma to the Loop Current by way of heat and volume transports through the Yucatan Channel. Figure 3 shows increased (model) volume and heat fluxes through the Yucatan Channel from Oct/18 to Oct/22 ~ 23. The increased fluxes are due to northwestward convergent flows produced while the storm is in the Caribbean Sea. Subsequent variation (after Oct/23) consists of damped near-inertial oscillations in which the volume fluxes asymptote to pre-Wilma values, and the upper-150m heat flux indicates influx of cooled (i.e., negative heat flux) Caribbean Sea waters (previously observed at 42056; Figure 2b) into the Gulf. Excess (i.e., control minus auxiliary run A1) of total transport (blue curves) averaged over Oct/19 ~ 23 is 2 Sv, and the excess transport in the surface 150 m (red) is  $\approx 5$  Sv, indicating a large baroclinic response with opposite transport below 150m (green). The fluxes peak on Oct/22 ~ 23 when currents in the western Yucatan Channel become very strong ( $\approx 2.3$  m s<sup>−1</sup>) forced by strong northward wind in the channel as Wilma stalled over the northern Yucatan Peninsula. In contrast, pre-storm current speeds are weaker, about 1.5 m s<sup>−1</sup> as inferred from the model and also from an observed drifter (available at www.aoml.noaa.gov/phod/dataphod) (Figure 1). In Figure 4 we plot the *SST* difference (at  $z = -1$  m), control minus

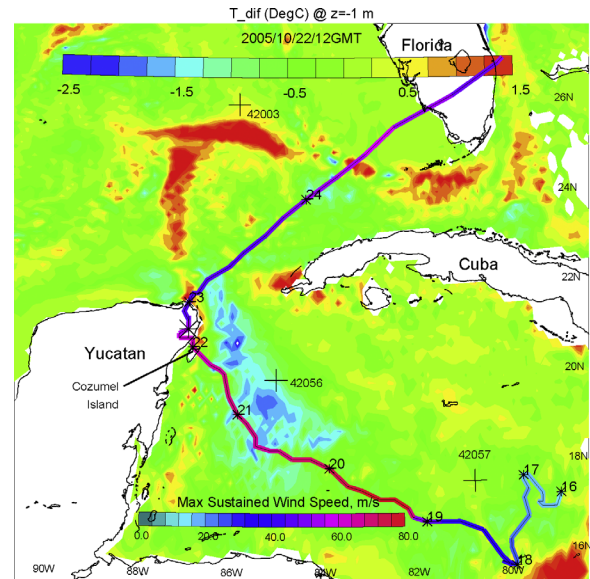


**Figure 4.** Color image of the temperature difference (°C; color-scale across top), control minus auxiliary run A1, on Oct/22/12GMT and at  $z = -1$  m, showing the effect of Wilma winds in warming the Loop Current especially around the edge of the Loop. Maximum *SST*-rise in the Loop was 2.18°C, minimum *SST*-drop off Cozumel is −2.85°C. Wilma's path and NDBC stations are also shown, same as in Figure 1.



auxiliary run A1, on Oct/22/12GMT. (Subtracting the A1-solution minimizes contributions from background variability that is not related to Wilma. However, the general warming in the Loop and cooling in the Caribbean in Figure 4 remain if the initial condition is subtracted instead.) This shows warming (red) around the edge of the Loop where currents are strong and cooling (blue) in the Caribbean Sea to the right of Wilma's path (Figure 2b). The asymmetry is striking. The warming is in part caused by localized wind-induced convergences especially at fronts, but a large part is by excess influx of warmer waters from the Caribbean. (To isolate localized advection by wind, a case that uses Wilma's wind field at the northern tip of Yucatan (on Oct/23) was run. We found  $SST$ -rise  $\approx 0.3^\circ\text{C}$  in the Loop, or about 20% of the total shown in Figure 4.) Based on the excess heat influx (the Oct/18–23 average is  $1.2 \times 10^7 \text{ }^\circ\text{C m}^3 \text{ s}^{-1}$  (or  $5 \times 10^{13} \text{ W}$ ), Figure 3) heat balance in an adiabatic stream-tube around the Loop Current (75 km wide  $\times$  150 m deep  $\times$  400 km long) from Oct/18 to 23 is computed; this yields an average increase of  $1^\circ\text{C}$  in agreement with Figure 4. The Yucatan-Loop Current system plays an important role in distributing the heat far north into the Gulf (around the Loop); in their absence, warming occurs only near the channel. This was confirmed by forcing Wilma onto an initially quiescent ocean with level isopycnals. The surface then cannot show warming because there are no horizontal thermal gradients (and no surface heat flux), but there is subsurface warming of about  $0.5^\circ\text{C}$  at  $z = -50 \text{ m}$ , caused by flow convergence, close to the channel mouth.

#### 4. Discussion

[11] We have computed geostrophic transports through the Yucatan Channel based on satellite altimetry data (*OASSH*; not shown). Prior to Wilma's entrance into the Gulf, the data shows an increased transport that is consistent with the model forecast shown in Figure 3, and the *OASSH* averaged over the Loop also increased. These data provide a tentative support of the warming episode observed at buoy 42003. Also, the model shows large subsurface (i.e.,  $z < -150 \text{ m}$ ) transport into the Gulf days after Wilma has passed (Figure 3, green curve). Subsurface influx encourages Loop Current extension [Hurlburt and Thompson, 1980], and both model and *OASSH* maps show a more extended Loop following Wilma. The extension may be a response to the increased transport [Ezer *et al.*, 2003], or (and) to the production of higher potential vorticity [Oey, 2004] by the intense cyclone that developed in the western portion of the Yucatan Channel when Wilma entered the Gulf.

#### 5. Conclusion

[12] Summarizing, cooling was observed at a buoy hundreds of kilometers from, and days ahead of hurricane

Wilma in the northwestern Caribbean Sea. A buoy in the northern edge of the Loop Current recorded  $SST$ -rise a few days prior to Wilma's entrance into the Gulf. The model study indicates that the rise was part of an overall warming around the Loop due in part to an increased influx of warm water into the Gulf of Mexico while Wilma was in the Caribbean Sea. Hurricane intensity is sensitive to slight changes in  $SST$  [Emanuel, 2005]. Results presented here suggest that hurricane predictions may benefit from prognostic ocean forecasts that have realistic representations of strong flows such as the Loop Current (and eddies).

[13] **Acknowledgments.** We are grateful to the Minerals Management Service and the Office of Naval Research for support. Computing was done at NOAA/GFDL.

#### References

- Caplan, P., J. Derber, W. Gemmill, S.-Y. Hong, H.-L. Pan, and D. Parrish (1997), Changes to the 1995 NCEP operational medium-range forecast model analysis-forecast system, *Weather Forecasting*, **12**, 581–594.
- Chelton, D. B., R. A. deSzoeke, M. G. Schlax, K. E. Naggar, and N. Siwertz (1998), Geographical variability of the first baroclinic Rossby radius of deformation, *J. Phys. Oceanogr.*, **28**, 433–460.
- Emanuel, K. A. (2005), *Divine Wind—The History and Science of Hurricanes*, Oxford Univ. Press, New York.
- Ezer, T., L. Oey, H. Lee, and W. Sturges (2003), The variability of currents in the Yucatan Channel: Analysis of results from a numerical ocean model, *J. Geophys. Res.*, **108**(C1), 3012, doi:10.1029/2002JC001509.
- Geisler, J. E. (1970), Linear theory of the response of a two-layer ocean to a moving hurricane, *Geophys. Fluid Dyn.*, **1**, 249–272.
- Hurlburt, H. E., and J. D. Thompson (1980), A numerical study of Loop Current intrusions and eddy shedding, *J. Phys. Oceanogr.*, **10**, 1611–1651.
- Large, W. G., and S. Pond (1981), Open ocean flux measurements in moderate to strong winds, *J. Phys. Oceanogr.*, **11**, 324–336.
- Leipper, D. F., and D. Volgenau (1972), Hurricane heat potential of the Gulf of Mexico, *J. Phys. Oceanogr.*, **2**, 218–224.
- Oey, L. (2004), Vorticity flux through the Yucatan Channel and Loop Current variability in the Gulf of Mexico, *J. Geophys. Res.*, **109**, C10004, doi:10.1029/2004JC002400.
- Oey, L.-Y., T. Ezer, and H. J. Lee (2005a), Loop Current, rings and related circulation in the Gulf of Mexico: A review of numerical models and future challenges, in *Circulation in the Gulf of Mexico: Observations and Models*, *Geophys. Monogr. Ser.*, vol. 161, edited by W. Sturges and A. Lugo-Fernandez, 360 pp., AGU, Washington, D. C.
- Oey, L.-Y., T. Ezer, G. Forristall, C. Cooper, S. DiMarco, and S. Fan (2005b), An exercise in forecasting loop current and eddy frontal positions in the Gulf of Mexico, *Geophys. Res. Lett.*, **32**, L12611, doi:10.1029/2005GL023253.
- Powell, M. D., P. J. Vickery, and T. Reinhold (2003), Reduced drag coefficient for high wind speeds in tropical cyclones, *Nature*, **422**, 279–283.
- Price, J. F. (1981), Upper ocean response to a hurricane, *J. Phys. Oceanogr.*, **11**, 153–175.
- Shay, L. K., G. J. Goni, and P. G. Black (2000), Effects of a warm oceanic feature on Hurricane Opal, *Mon. Weather Rev.*, **128**, 1366–1383.
- Turner, J. S. (1973), *Buoyancy Effects in Fluids*, 367 pp., Cambridge Univ. Press, New York.

T. Ezer, L.-Y. Oey, and X.-Q. Yin, Atmospheric and Oceanic Sciences, Princeton University, P.O. Box CN 710, Sayre Hall, Princeton, NJ 08544, USA. (lyo@princeton.edu)

S.-J. Fan, Stevens Institute of Technology, Hoboken, NJ 07030, USA.  
D.-P. Wang, Marine Sciences Research Center, Stony Brook University, 167 Endeavour Hall, Stony Brook, NY 11794-5000, USA.